Proceedings of 7th Transport Research Arena TRA 2018, April 16-19, 2018, Vienna, Austria

Contact Pressure Measurement of a Small-Scale Wheel Tracking Device for Different Surface Types

Dermot B. Casey a*, James R. Grenfell b, Gordon D. Airey c, Phillip Millar d, and David Woodward e

[a]*AECOM, 12 Regan Way, Beeston, Nottingham, NG9 6RZ, UK*
[b]*arrb, 500 Burwood Hwy, Vermont South, IVC 3133, Australia*
[c]*Nottingham Transportation Engineering Centre (NTEC), University of Nottingham, University Park, Nottingham, UK*
[d,e]*Belfast School of Architecture and the Built Environment, University of Ulster, Shore road, Newtonabbey, Co. Antrim, BT37 0QB, UK*

Abstract

In pavement engineering design, the pressure under a tyre is assumed to be a circular vertical contact pressure for analytical design methods. The true contact pressure and area is very difficult to predict due to the complexity of the system. A normal test that is undertaken to understand an asphalt's performance for near surface rutting is the small-scale wheel tracker. The contact pressure and area of the tyre for different loads and surface types is not known. This is an area that needs to be addressed to better understand the contact pressures in this crucial test for asphalt rutting. Different pavement surface material slabs were made all with different surface textures for testing in the small-scale wheel tracker. A device was chosen to measure contact pressure between the tyre and these different surfaces. The device deforms around the surface aggregates and gives a very good understanding of the forces between the tyre and the pavement surface. It was shown that there is a great deal of variability between the different surface types. It is recommended that pavement loading for design should have a factor based on the contact pressure characteristics of a pavement surface.

Keywords: small wheel tracker; pavement distress; tyre-pavement; contact pressure; skid resistance; wear;

* Corresponding author.
E-mail address: dermot.casey@aecom.com

1. Introduction

In pavement engineering design, the pressure under a tyre is assumed to be a circular vertical contact pressure for analytical design methods. However, the contact pressure shape and stress components are dependent on the complex mixture of tyre type, inflation (if pneumatic tyre), loading and surface texture of the pavement. The true contact pressure and area is very difficult to predict due to the complexity of the system. The best solution is to measure the contact pressure between a tyre and a pavement surface. Several methods exist to measure contact pressure of tyres a lot of these methods have limitations that either make them cumbersome to use or use an idealised pavement surface. The contact pressure and area variation probably does not have a large influence on the traditional areas of pavement distress (fatigue cracking at the bottom of the asphalt and rutting on top of the subgrade) as the contact pressure evens out through the pavement. The areas where these complex contact pressure have an influence on pavement performance are in the near surface (cracking and rutting) and the skid resistance of the aggregates.

A normal test that is undertaken to understand an asphalt's performance for near surface rutting is the small-scale wheel tracker which consists of a solid rubber tyre and known load running over a slab of asphalt at a known temperature and speed. An important piece of information is not known though, the contact pressure and area of the tyre for different loads and surface types. This is an area that needs to be addressed to better understand the contact pressures in this crucial test for asphalt rutting.

Three objectives were formulated to address this issue:

- To manufacturer different pavement surface material slabs all with different surface textures for testing in the small-scale wheel tracker.
- Measurement of the tyre-pavement contact pressure by means of a deformable measuring mat that fits between the surface of the materials and the small-scale wheel tracker wheel.
- Analysis of the results of the contact pressure measurement for different materials and processing of the statistical significance of these results.

2. Background

True tyre contact pressure is composed of non-uniform vertical, transverse and longitudinal contact pressures. The largest component of stress is the vertical contact pressure and it is this that has the largest influence on pavement behaviour (Pottinger, 1992; De Beer et al, 1997; Myers et al., 1999; Blab, 1999; Fernando et al., 2006; Wang & Roque, 2010). The non-uniform contact pressure is in stark contrast to the representation of contact pressure as a uniform circular contact pressure in current design methods (Powell et al., 1984; Theyse et al., 1996). It is shown that these non-uniform contact pressures are of importance to the behaviour of pavements especially on the surface and near surface (Siddharthan and Sebaaly, 1998; Perret, 2002; Novak et al., 2003a; Park et al., 2005; Luo and Prozzi, 2006). The conditions that are created in the near surface are greatly different from these for uniform conditions and could lead to rutting and cracking in these regions (Perret, 2002; Luo and Prozzi, 2006; Al-Qadi and Wang, 2012). It has been shown that there are significant differences to surface cracking potential caused by non-uniform contact pressure (Collop and Cebon, 1995; Casey et al., 2012; Casey et al., 2014).

The magnitude of these non-uniform contact pressures has been shown to be highly influenced by the tyre type, tyre loading and inflation pressure (Marshek, et al., 1985; Pottinger. 1992; De Beer et al., 1997; Blab, 1999; De Beer et al., 1999; Novak et al., 2003b; Fernando et al., 2006; Douglas et al., 2008; Wang & Roque, 2010, Woodward et al., 2013). An individual tyre can have a large range of vertical contact pressure depending on the inflation pressure and tyre loading (Prozzi and Luo, 2005, Fernando et al., 2006). The majority of the studies presented here use an instrumented idealised asphalt surface to measurement contact pressure. Therefore, they are not measuring the contact pressure between a real surface and a tyre. A device was chosen to measure contact pressure between the tyre and these different surfaces. The device used was a flexible piezo-electric pressure mat with very dense resolution. The device deforms around the surface aggregates and gives a very good understanding of the forces between the tyre and the pavement surface. The contact pressure areas can also be calculated by using the influence area of each measuring point that is in contact with the tyre and the pavement surface. This will give a better insight into the contact pressure between a tyre and the pavement without having to idealised the pavement surface by turning it into a measuring device.

3. Methodology

The experiments for this study took place on the Cooper technology small tracking device at NTEC (Nottingham Transportation Engineering Centre) at the University of Nottingham. This machine is used to identify the rut susceptibility of asphalt mixtures by tracking a solid rubber tyre across the sample surface at different temperatures for a number of repetitions until a set amount of defomration has taken place. The loading arm was set in the British Standard (BS) wheel tracking testing position and the BS loading was used for a portion of the experiments. The wheel was held in a static position for the measurement of contact pressure on the 6 different samples that were tested.

Table 1. The different types of samples used to measure contact pressure

Sample description and contact pressure measured
6 mm (max aggregate size) stone mastic asphalt (SMA)
14 mm (max aggregate size) stone mastic asphalt (SMA)
20 mm (chipping size) Under-chipped hot rolled asphalt (HRA)
14 mm (max aggregate size) asphalt concrete (AC)
Unchipped hot rolled asphalt (HRA)
Smooth Steel without texture

The six samples listed show a diverse cross-section of different types of surface finish (Table 1 and Figure 1). There are samples that have positive texture (under-chipped HRA), negative texture (SMA and AC) and two that have relatively smooth finishes (unchipped HRA and the Smooth Steel). This will allow for a comparison to be made between the different materials and the contact pressure they create between their surface and the small wheel tracker static wheel.

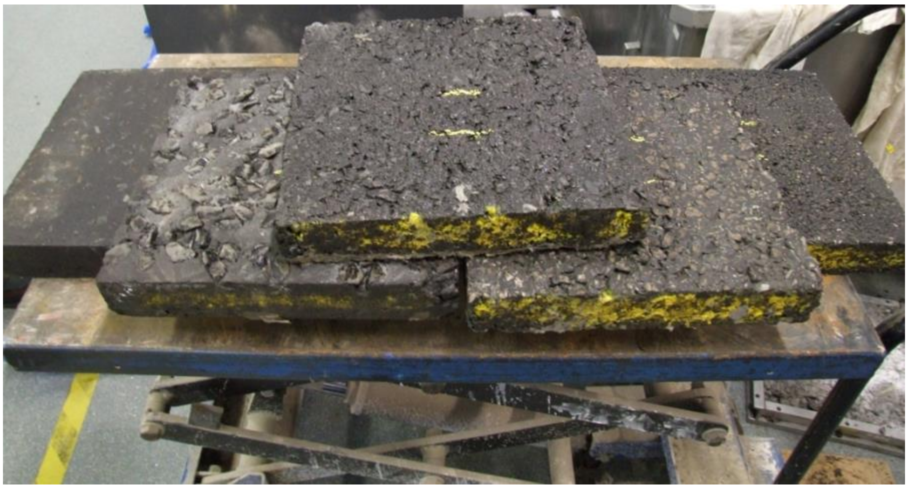

Figure 1. Asphalt samples tested from left to right: Unchipped HRA, Under-chipped HRA, 14 mm AC, 14 mm SMA and 6 mm SMA.

The contact pressure was measured by the University of Ulster using the Xsensor flexible pressure mat which has a diverse range of applications from a patient's pressure points in a bed to the automotive industry. The mat is a flexible rubber membrane with a matrix of pressure cells (the one used in this study the grid is at 2.57 mm centres). This mat can be placed between two objects and the forces between the two bodies can be measured. The device also allows the contact area between the two bodies to be measured for comparison by using the number of points loaded and the influence area of these points. The forces and the influence area are then combined to the contact pressure for each measurement point. The test set-up consisted of placing the sample on the test steel loading platen then lowering the wheel on to the slab and marking the position. The wheel was then raised and the flexible pressure mat was placed on the slab (Figure 2) and the wheel was lowered again. 100 readings of the contact pressure were then captured per test combination. This was to eliminate any inaccuracy that could be caused by settling on the device. These values were post-processed to give single numbers for each test combination. Each sample was measured with no loading (there is still loading from the self-weight of the arm and wheel) and with BS loading in the same way as described here.

Figure 2. Test set-up with the small wheel track up and the flexible pressure mat over the sample

All the samples were measured for unloaded and BS loaded conditions using the test set-up described. This gave a large quantity of information that needed to be sorted and processed to give descriptive statistics of how the nature of contact pressure is different for each test combination. The results of this can be seen in the next section.

4. Results and Discussion

The contact pressure between the surface of each sample and the small wheel tracker was recorded for the loaded and unloaded conditions. The statistics of these combinations were extracted from the sensor readings after post-processing. These values show how the values change for the different surface types and loading conditions (Table 2).

Table 2. A list of the key statistics for the 6 sample types and 2 loading conditions for the small wheel tracking device

	Smooth Steel		Unchipped HRA		6 mm SMA		14 mm SMA		Under-chipped HRA		14 mm AC	
	Unloaded	Loaded	Unloaded	Loaded	Unloaded	Loaded	Unloaded	Loaded	Unloaded	Loaded	Unloaded	Loaded
Average (kPa)	210	345	209	365	271	390	294	367	250	429	280	466
Min (kPa)	12	12	12	24	11	12	12	12	12	12	12	23
Max (kPa)	406	628	452	901	1039	1765	1607	1765	1765	1765	1361	1765
Stdev (kPa)	119	182	113	154	181	277	350	370	333	414	266	411
Area (mm2)	1000	1277	903	1097	697	1006	626	1019	781	961	716	942

The unloaded average contact pressure varies from 209 (unchipped HRA) to 294 kPa (14 mm SMA). This shows a large spread across the different sample types with it being nearly one third of the lowest average. The loaded average varies from 345 (smooth steel) to 466 kPa (14 mm AC). This is a large spread across the different samples and proportionally very like the unloaded scenario. The interesting aspect of this is that there is an interchange of ranking depending on the loading scenario (Table 2). The contact of each sample increases with loading but so too does the average contact pressure. This shows that the contact area grows with the increase in loading but not proportionally. There is a plateauing of the contact area at the higher average contact pressure loading. The maximum value that the sensor outputs is 1765 kPa and this is reached for four of the samples (loaded), this is all the samples with a texture. An interesting observation is that the 14 mm SMA and AC are both negative texture surface finishes and have similar average contact pressure for the unloaded condition (294 and 280 kPa respectively) but for the loaded condition there is a big change (367 and 466 kPa).

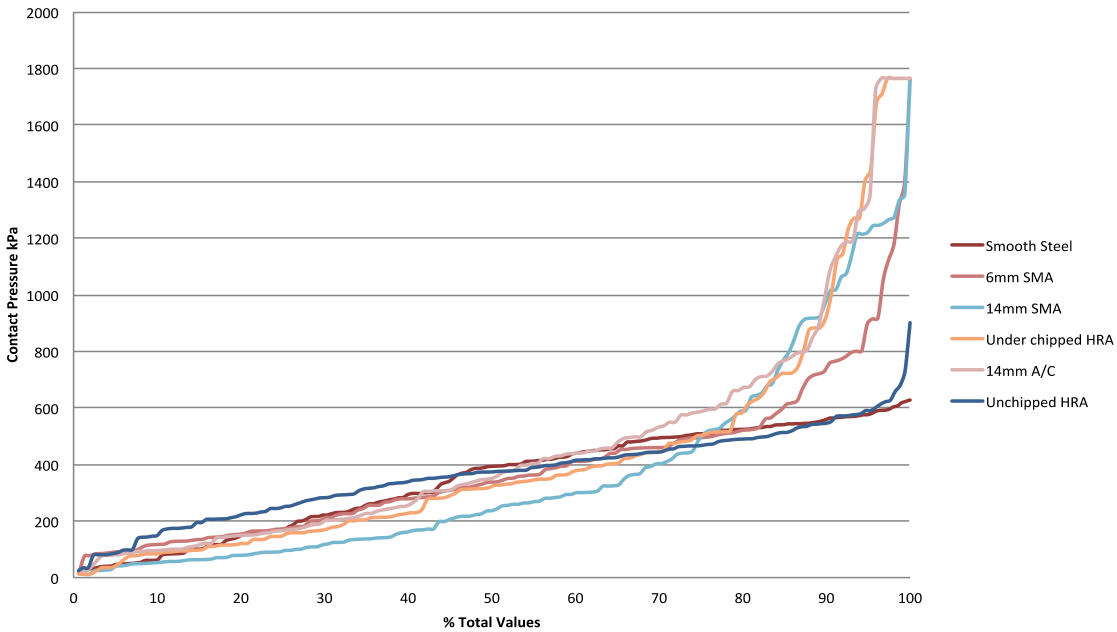

Figure 3. The cumulative frequency of contact pressure values for the different samples loaded

It can be seen that there is a relative linear relationship between the percentage of values and contact pressure up to 70 % and 500 kPa (Figure 3). However, after these values the is a divergence of behaviour between the smooth steel and unchipped HRA and the rest of the samples. There is a rapid increase in contact pressure measurements after this point for the other four samples showing how the texture of these samples creates areas of high contact pressure. The samples with the greatest frequency of high contact pressure measurements is the under-chipped HRA and 14 mm AC reflecting their high average contact pressure (Table 2). Given the same aggregate type it is probable that the samples with the highest contact pressures will wear quicker and lose skid resistance quicker as they become polished. This is significant for the specification of a particular surface type for the whole life costing of that material.

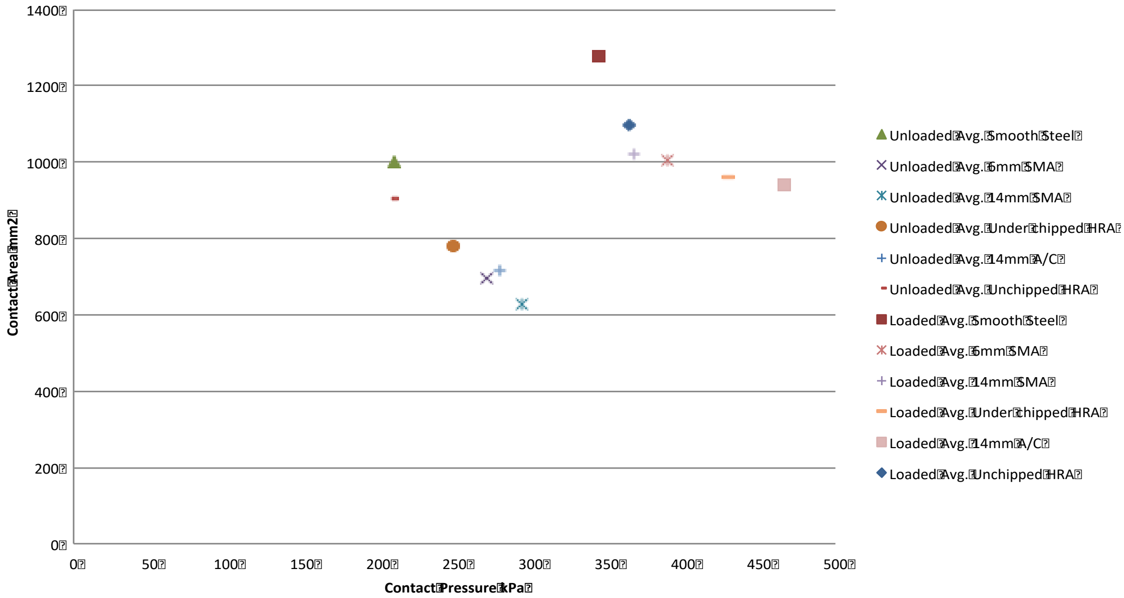

Figure 4. Contact area vs. Average contact pressure for all the samples loaded and unloaded

The contact pressure vs. the contact area show two distinct groupings for the loaded and unloaded conditions (Figure 4). There is good alignment in this groups of both average contact pressure increasing with increased contact area. The unloaded grouping has an R^2 value of 0.93 and the loaded has an R^2 of 0.63. This difference is probably due to the 4 loaded textured samples levelling off on contact area but the average contact pressure continuing to increase. This limiting of the contact pressure to the loading is probably linked to the deformation characteristics of the rubber of the loading wheel.

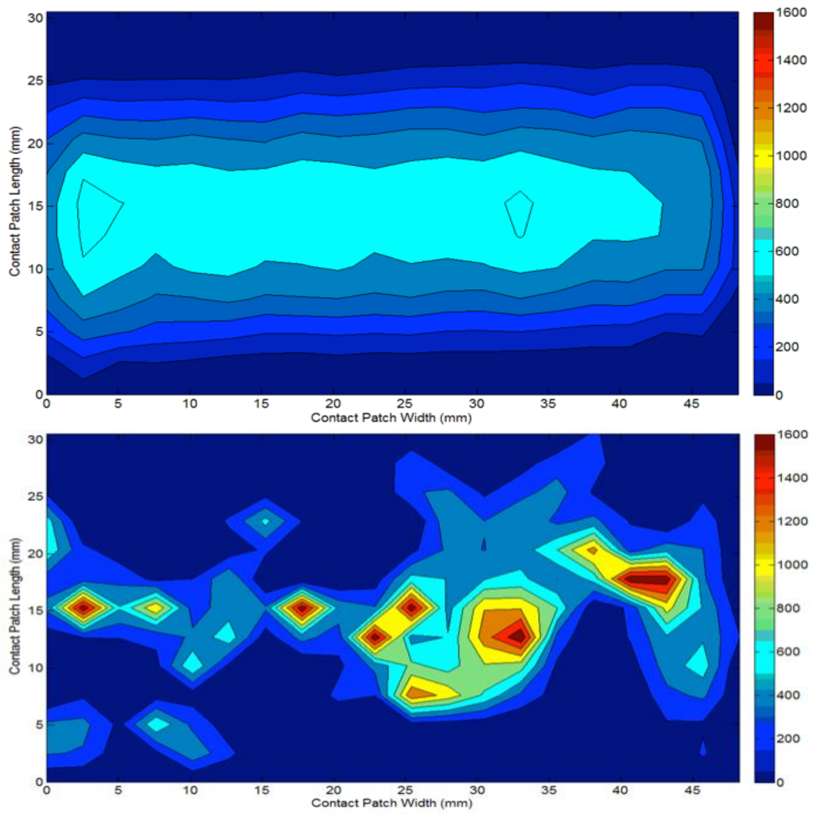

Figure 5. The contact pressure (kPa) for the Smooth steel sample (top) and for the 14 mm AC (bottom) loaded

It is shown that there is a great difference between the distribution of contact pressure for the smooth steel and 14 mm AC (Figure 5). The smooth steel has a hertzian contact pressure distribution whereas the 14 mm AC has peaks on the aggregates. These aggregates have very high contact pressures with areas in between having very low contact pressure. This would mean that as a tyre passes over this material these aggregates will be continuously subjected to high contact pressure wearing the aggregates and damaging the surface. The contact pressure of the tyre will be transmitted to the pavement via this small high pressure contact patch.

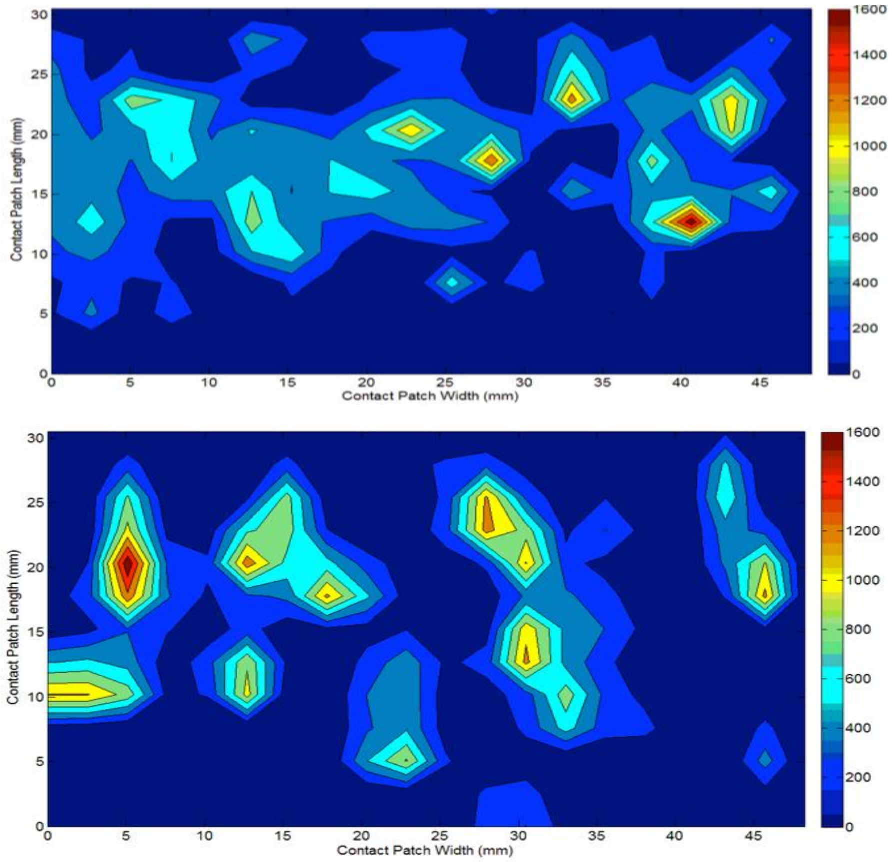

Figure 6. The contact pressure (kPa) for the 6 mm SMA sample (top) and for the 14 mm SMA (bottom) loaded

The comparison of the 6 and 14 mm SMA is interesting as it shows that for the same asphalt mix but with different maximum aggregate size the different distribution of contact pressure (Figure 6). The use of a smaller stone size distributes the contact pressure more evenly across the surface. This creates smaller peaks in contact pressure. This would mean these aggregates are more evenly worn and should have a longer service life. The 6 mm stone would have higher laying cost but in the long term could be less expensive due to an increased service life.

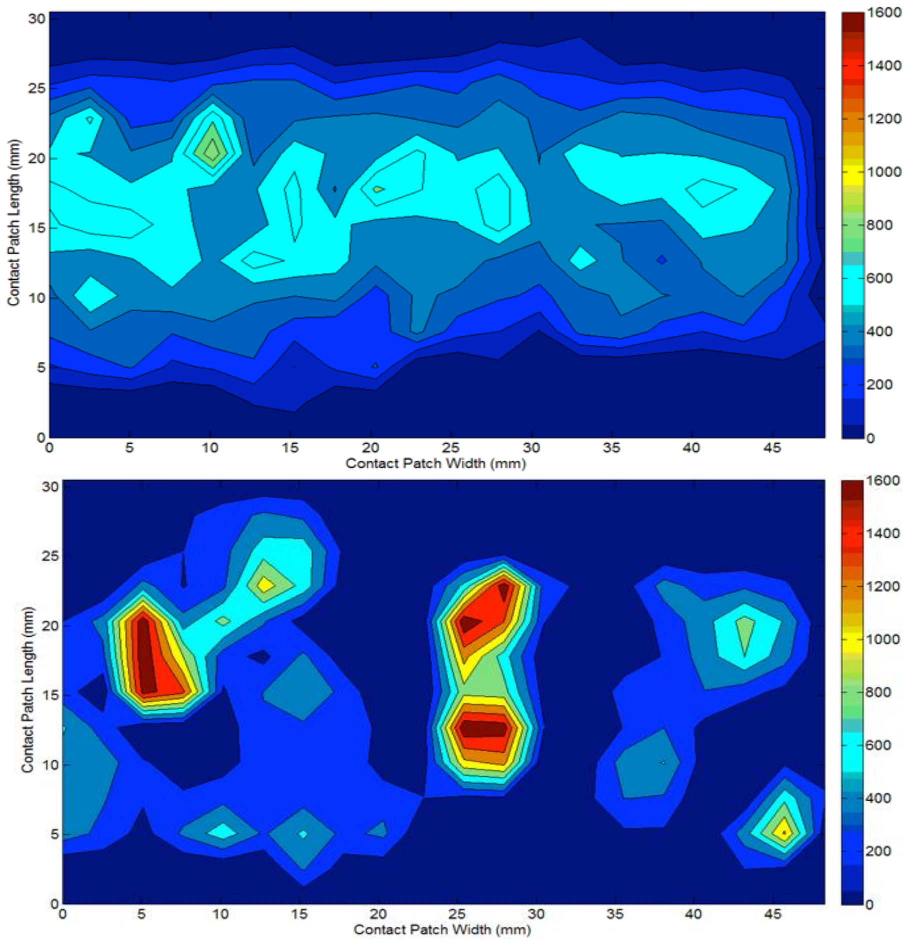

Figure 7. The contact pressure (kPa) for the unchipped HRA sample (top) and for the 20 mm under-chipped HRA (bottom) loaded

It is interesting to note the difference between the two HRA samples (Figure 7). The unchipped sample shows some minor peaks of contact pressure probably due to the slightly uneven surface achieved of the sample. The under-chipped on the under hand has three pieces of aggregate where there are very high peaks in contact pressure. The chippings completely change the nature of the contact pressure. This would wear these 3 stones disproportionately quicker than the rest of the surface. This would mean that in addition to providing too few stones and possibly inadequate skid resistance to start with the rate of the decrease in skid resistance would be more rapid.

The themes in the study are that the larger aggregate sizes give the highest average contact pressure values for the loaded scenario. The 14 mm AC and 20 mm under-chipped HRA give the highest values and it would be expected these would wear quicker due to this. The next highest is the 14 mm SMA which has a significantly lower average contact pressure compared to the 14 mm AC. This shows that the same maximum aggregate can have very different contact pressure. The 6 mm SMA was the best performing of the textured samples with the contact pressure spread over more small aggregates and therefore giving a lower average contact pressure. The smooth steel and unchipped HRA showed a similar average contact pressure but the smooth steel having a larger contact area when loaded. These results will not only have a bearing on the wear of the aggregates but the surface and near surface structural performance of the pavement. If the wheel load is transmitted into the pavement over a smaller area with higher contact pressure this will lead to an increased accumulation of damage in the form of cracking and rutting. It is generally true that smaller maximum aggregate size asphalt is more expensive than larger but it could be the case that over time with reduced rates of accumulation of distress the pavement has a longer service life. This would reduce the whole life cost of the pavement.

5. Conclusions

The information presented in this paper is focused on understanding the nature of contact pressure between the small wheel tracker and different pavement surfaces for loaded and unloaded scenarios. The results and discussion lead to several conclusions being drawn from this work.

- The loaded scenario compared to the corresponding unloaded scenario has higher average contact pressure and greater contact area for all samples.
- The textured samples have the highest proportion of high contact pressure measurements relative to the total number of contact pressure measurements.
- The average contact pressure is highest for a 14 mm AC followed by a 20 mm under-chipped HRA for the loaded condition. This would suggest that these two would wear more quickly than the other samples for skid resistance and near surface distress.
- The 14 mm SMA has an average contact pressure nearly 100 kPa lower than for the 14 mm AC. This shows it is not just maximum aggregate size that influences the contact pressure.
- The textured sample with the lowest average contact pressure is the 6 mm SMA showing that the smaller aggregate size can reduce the contact pressure by spreading the contact pressure over more points with lower peak values lowering the rate of wear and near surface distress. This could help to increase the service life of this material compared to the other textured samples and give it a better whole life cost.

6. References

Al-Qadi, I., & Wang, H., 2012. Impact of Wide-Base Tires on Pavements. Transportation Research Record: Journal of the Transportation Research Board, 2304(-1), 169-176.

Blab, R., 1999. Introducing Improved Loading Assumptions into Analytical Pavement Models Based on Measured Contact Stresses of Tires. Paper presented at the International Conference on Accelerated Pavement Testing, Reno, NV, USA.

Casey, D. B., Collop, A. C., Grenfell, J. R., & Airey, G. D., 2012. Stress Intensity Factors at the Tip of a Surface Initiated Crack Caused by Different Contact Pressure Distributions. Procedia-Social and Behavioral Sciences, 48, 733-742.

Casey, D. B., Grenfell, J. R., & Airey, G. D., 2014. 3-D longitudinal and transverse cracking and the influence of non-uniform contact pressure on the stress intensity factors of these Cracks. In Transport Research Arena (TRA) 5th Conference: Transport Solutions from Research to Deployment.

Collop, A. C., & Cebon, D., 1995. A theoretical analysis of fatigue cracking in flexible pavements. Proceedings of the Institution of Mechanical Engineers. Part C, Mechanical engineering science., 209(5), 345.

De Beer, M., Fisher, C., & Jooste, F. J., 1997. Determination of pneumatic tyre/pavement interface contact stresses under moving loads and some effects on pavements with thin asphalt surfacing layers. In Proceedings of the 8th International Conference on Asphalt Pavements, Seattle, Washington, USA (Vol. 1, pp. 10-14).

De Beer, M., Kannemeyer, L., & Fisher, C., 1999. Towards improved mechanistic design of thin asphalt layer surfacings based on actual tyre/pavement contact stress - in - motion (sim) data in south africa. 7th conference on asphalt pavements for Southern Africa, South Africa.

Douglas, R., Alabaster, D., & Charters, N., 2008. Measured Tire-Road Contact Stresses Characterized by Tire Type, Wheel Load, and Inflation Pressure. Paper presented at the 2008 Annual Conference of the Transportation Association of Canada, Toronto, Ontario, Canada.

Fernando, E. G., Musani, D., Park, D. W., & Liu, W., 2006. Evaluation of effects of tire size and inflation pressure on tire contact stresses and pavement response (No. FHWA/TX-06/0-4361-1).

Luo, R., & Prozzi, J. A., 2006. Pavement responses at asphalt surface under measured 3-d tire-pavement contact stresses. University of Texas, Texas, USA.

Marshek, K. M., Hudson, W. R., Connell, R. B., Chen, H., & Saraf, C., 1985. Experimental investigation of truck tire inflation pressure on pavement-tire contact area and pressure distribution: Center for Transportation Research, the University of Texas at Austin, Texas, USA.

Myers, L. A., Roque, R., Ruth, B. E., & Drakos, C., 1999. Measurement of Contact Stresses for the Different Truck Tire Types to Evaluate their Influence on Near-Surface Cracking and Rutting. Transportation Research Record(1655), p. 175-184.

Novak, M., Birgisson, B., & Roque, R., 2003a. Tire Contact Stresses and Their Effects on Instability Rutting of Asphalt Mixture Pavements: Three-Dimensional Finite Element Analysis. Transportation Research Record: Journal of the Transportation Research Board, 1853(-1), 150-156.

Novak, M., Birgisson, B., & Roque, R., 2003b. Near-surface stress states in flexible pavements using measured radial tire contact stresses and ADINA. Computers & Structures, 81(8-11), 859-870.

Park, D.-W., Fernando, E., & Leidy, J., 2005. Evaluation of Predicted Pavement Response with Measured Tire Contact Stresses. Transportation Research Record: Journal of the Transportation Research Board, 1919(-1), 160-170.

Perret, J., 2002. The effect of loading conditions on pavement responses calculated using a linear-elastic model. Paper presented at the Proceeding of the 3rd International Symposium on 3D Finite Element for Pavement Analysis, Design and Research (283-303).

Pottinger, M., 1992. The three-dimensional contact patch stress field of solid and pneumatic tires. Tire Science and Technology, 20(1), 3-32.

Powell, W. D., Potter, J. F., Mayhew, H. C., & Nunn, M. E. (1984). The structural design of bituminous roads (No. LR 1132 Monograph).

Prozzi, J. A., & Luo, R., 2005. Quantification of the joint effect of wheel load and tire inflation pressure on pavement response. Transportation

Research Record.(1919), 134-141.

Siddharthan, R. V., Yao, J., & Sebaaly, P. E., 1998. Pavement strain from moving dynamic 3D load distribution. Journal of Transportation Engineering-Asce, 124(6), 557-566.

Theyse, H. L., De Beer, M., & Rust, F. C., 1996. Overview of South African mechanistic pavement design method. Transportation Research Record: Journal of the Transportation Research Board, 1539(1), 6-17.

Wang, G., & Roque, R., 2010. Three-Dimensional Finite Element Modeling of Static Tire-Pavement Interaction. Transportation Research Record: Journal of the Transportation Research Board, 2155(-1), 158-169.

Woodward, D., Millar, P., Friel, S. & Waddell, C., 2013. Measuring Grip and the Contact Patch. In Airfield and Highway Pavement 2013: Sustainable and Efficient Pavements (pp. 841-854).